ANTIOXIDANTS & REDOX SIGNALING
Volume 31, Number 9, 2019

DOI: 10.1089/ars.2018.7693

Redox-Dependent Loss of Flavin by Mitochondrial Complex I in Brain Ischemia/Reperfusion Injury

Anna Stepanova,[1] Sergey Sosunov,[1] Zoya Niatsetskaya,[1] Csaba Konrad,[2] Anatoly A. Starkov,[2] Giovanni Manfredi,[2] Ilka Wittig,[3,4] Vadim Ten,[1] and Alexander Galkin[1]

Abstract

Aims: Brain ischemia/reperfusion (I/R) is associated with impairment of mitochondrial function. However, the mechanisms of mitochondrial failure are not fully understood. This work was undertaken to determine the mechanisms and time course of mitochondrial energy dysfunction after reperfusion following neonatal brain hypoxia-ischemia (HI) in mice.
Results: HI/reperfusion decreased the activity of mitochondrial complex I, which was recovered after 30 min of reperfusion and then declined again after 1 h. Decreased complex I activity occurred in parallel with a loss in the content of noncovalently bound membrane flavin mononucleotide (FMN). FMN dissociation from the enzyme is caused by succinate-supported reverse electron transfer. Administration of FMN precursor riboflavin before HI/reperfusion was associated with decreased infarct volume, attenuation of neurological deficit, and preserved complex I activity compared with vehicle-treated mice. *In vitro*, the rate of FMN release during oxidation of succinate was not affected by the oxygen level and amount of endogenously produced reactive oxygen species.
Innovation: Our data suggest that dissociation of FMN from mitochondrial complex I may represent a novel mechanism of enzyme inhibition defining respiratory chain failure in I/R. Strategies preventing FMN release during HI and reperfusion may limit the extent of energy failure and cerebral HI injury. The proposed mechanism of acute I/R-induced complex I impairment is distinct from the generally accepted mechanism of oxidative stress-mediated I/R injury.
Conclusion: Our study is the first to highlight a critical role of mitochondrial complex I-FMN dissociation in the development of HI-reperfusion injury of the neonatal brain. *Antioxid. Redox Signal.* 31, 000–000.

Keywords: ischemia/reperfusion injury, mitochondrial complex I, flavin mononucleotide, reverse electron transfer, secondary energy failure

Introduction

Perinatal hypoxia-ischemia (HI) is one of the leading causes of neonatal mortality (42). In survivors, HI encephalopathy is a major cause of permanent neurological disability and has an estimated lifetime cost-of-care that is more than 1 million U.S. dollars (15).

The brain is the most sensitive organ to oxygen and substrate deprivation. In animal models of ischemia-reperfusion (I/R) injury of mature and immature brain, the lack of substrates and oxygen first slows down mitochondrial respiration and depletes ATP and phosphocreatine content. This state is known as primary energy failure (8, 23, 45, 50, 54, 65). Timely restoration of cerebral blood flow through reperfusion is critical for survival, as it transiently recovers mitochondrial activity and replenishes high-energy phosphates. Within a few hours of reperfusion, mitochondrial respiration declines again, leading to a gradual depletion of ATP production, which manifests as a secondary energy failure. Molecular mechanisms of this biphasic process are not understood (38,

[1]Division of Neonatology, Department of Pediatrics, Columbia University, New York, New York.
[2]Feil Family Brain and Mind Research Institute, Weill Cornell Medicine, New York, New York.
[3]Functional Proteomics, SFB815 Core Unit, Medical School, Goethe University, Frankfurt, Germany.
[4]German Center for Cardiovascular Research (DZHK), Partner Site RheinMain, Frankfurt, Germany.

Innovation

The molecular details of mitochondrial complex I impairment during ischemia/reperfusion (I/R) brain injury are not known. We investigated a neonatal mouse model of regional hypoxia-ischemia cerebral injury and found that the decline in activity of complex I is due to the loss of its redox cofactor flavin mononucleotide (FMN) and can be prevented by administration of FMN precursor riboflavin. This mechanism of acute I/R-induced complex I impairment is distinct from the commonly accepted oxidative stress-mediated reperfusion injury. Our data suggest that retention of FMN by mitochondrial complex I may be a novel therapeutic strategy to prevent energy failure in cerebral I/R.

45, 66). Why after an initial recovery does oxidative phosphorylation fail again, despite availability of oxygen and substrates?

Several putative mechanisms have been suggested for I/R-induced brain mitochondrial damage (3, 48, 58). Most of the reported evidence has shown a decline in mitochondrial respiration supported by the substrates of NAD^+-dependent dehydrogenases (1, 7, 28, 57, 58). This respiration is mediated by mitochondrial complex I, a large, 45-subunit membrane protein containing noncovalently bound flavin mononucleotide (FMN) and 8 iron-sulfur clusters acting as redox centers. The structure of mammalian complex I has been resolved only recently (17, 75). Complex I is the most sensitive respiratory chain complex to I/R damage, but the mechanisms of its impairment are not known. Inhibition of complex I activity after brain HI or ischemia has been observed in several brain I/R models (2, 31, 49). In these experimental models, complex I-dependent respiration almost fully recovered on reperfusion, but it became depressed again within 1–6 h of reperfusion (2, 49, 58). In contrast to complex I, other components of the respiratory chain succinate dehydrogenase (complex II) and cytochrome *c* oxidase (complex IV) were found to be minimally or not affected by brain ischemia (4, 31, 33, 49). This indicates that the rest of the respiratory chain (complexes II-IV segment) is still capable of effective respiration on I/R.

Complex I is the only mitochondrial enzyme responsible for energy-linked NADH oxidation and regeneration of NAD^+ for catabolic processes (Krebs cycle, glycolysis, fatty acids oxidation, etc). The enzyme is also able to catalyze the opposite reaction of reverse electron transfer (RET) when a small fraction of electrons from succinate is driven by the membrane potential upstream to complex I toward NAD^+ (9). RET supports the highest rate of reactive oxygen species (ROS) generation in mitochondria, and complex I has been identified as the main site of ROS production (5, 11, 26, 36, 44, 49, 51, 61, 63, 71).

Here, we used a model of neonatal brain HI to investigate acute I/R-induced changes in the mitochondrial respiratory chain, concentrating on the molecular mechanisms of primary and secondary energy failure. Our results suggest a central role of complex I in the development of bioenergetic failure in I/R injury. We show that I/R induces loss of the flavin cofactor FMN from complex I, rendering the enzyme inactive. The molecular mechanism of FMN dissociation is over-reduction of flavin *via* RET, without an apparent effect on enzyme integrity. Administration of FMN precursor riboflavin reduces complex I inactivation and attenuates I/R brain injury. This previously undescribed phenomenon may represent the major molecular mechanism of I/R-induced mitochondrial impairment.

Results

Neonatal HI-reperfusion inactivates mitochondrial complex I

In this study, the Rice-Vannucci model of neonatal stroke (68) was used to induce HI brain damage in postnatal day 10 mice (46). In this experimental paradigm, HI-reperfusion generates an infarction of 44.4% ± 20.5% of the entire hemisphere as determined by triphenyltetrazolium chloride (TTC) staining (Fig. 1A, B). Righting and negative geotaxis reflexes performance 24 h later was significantly worse (sluggish) in HI mice compared with naive mice, indicating sensorimotor neurological deficits due to the developing tissue damage (Fig. 1C, D).

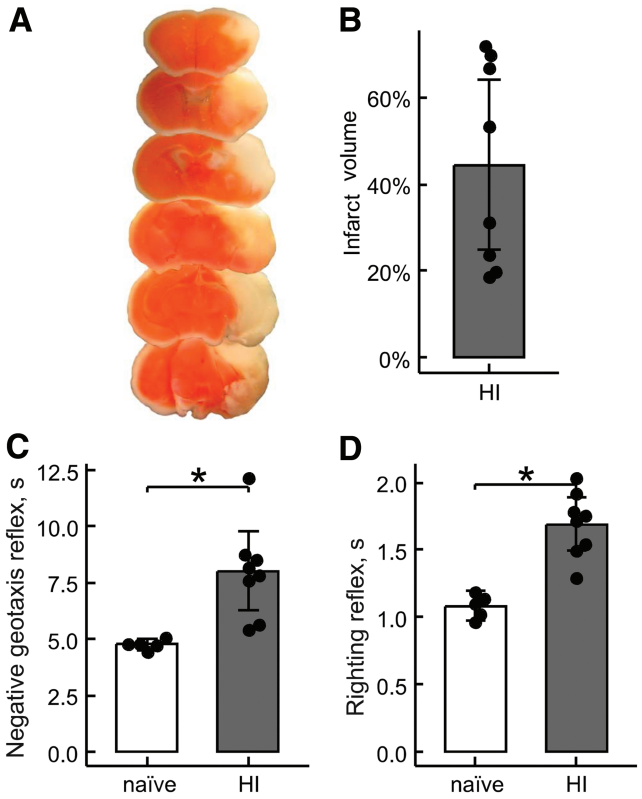

FIG. 1. Cerebral I/R injury after neonatal HI-reperfusion *in vivo*. (A) Infarct images obtained by TTC staining of coronal sections 24 h after HI-reperfusion. The normal tissue was stained (*red*), and the infarcted tissue was not stained (*white*). **(B)** Infarct volume as a percentage of the hemisphere; **(C, D)** negative geotaxis reflex (*left*), and righting (*right*) reflexes assessed 24 h after HI-reperfusion ($n = 5$–8 per group, $^*p < 0.05$, *t*-test). HI, hypoxia-ischemia; I/R, ischemia/reperfusion; TTC, triphenyltetrazolium chloride. Color images are available online.

We studied I/R-induced changes of mitochondrial function in this mouse model of neonatal HI-reperfusion. To assess complex I function, we measured two types of activities: physiological NADH:Q reductase and oxidation of NADH by the artificial acceptor hexaammineruthenium (III) (HAR). In contrast to the quinone, HAR takes electrons from the hydrophilic domain of complex I, most likely from the FMN, the first redox center of the enzyme (6, 59). This reaction is insensitive to the classical inhibitors of physiological activity of complex I, and it is typically used as the relative measure of functional complex I in the membrane (6, 35, 69). Compared with naive mice, complex I activity was significantly inhibited immediately after HI. At 15 min of reperfusion, however, complex I activity nearly fully recovered and then declined again at 1–2 h of reperfusion (Fig. 2A, B). Both physiological complex I activity and HAR reductase exhibited the same dynamics, which indicates that the HI/reperfusion-induced impairment takes place at the hydrophilic peripheral domain where FMN is bound [N-module, according to Hunte *et al.* (30)]. Other components of the respiratory chain, such as cytochrome *c* oxidase (complex IV) and succinate dehydrogenase (complex II), were only mildly affected (Fig. 2C, D), indicating that the rest of the respiratory chain was not significantly compromised.

Neonatal HI-reperfusion leads to the decline of noncovalently bound FMN content in mitochondrial membranes

Next, we studied the molecular basis of I/R-induced impairment of complex I. This multisubunit complex contains one molecule of noncovalently bound FMN per molecule of enzyme (17, 52, 75). We have found that HI-insult affected the functionality of the N-module of complex I where FMN is bound. The content of noncovalently bound FMN in mitochondria isolated from the brain after HI-reperfusion (Fig. 2E) coincides with changes in complex I activities measured in the same preparation (Fig. 2A, B). Since flavin is a direct acceptor of electrons from NADH, the FMN-deficient enzyme is unable to catalyze either physiological NADH:Q or artificial NADH:HAR reductase reactions (25, 29, 61). Therefore, we concluded that complex I impairment after HI-reperfusion was, indeed, due to a loss of FMN by the enzyme.

Succinate-supported RET results in dissociation of FMN from mitochondrial complex I

Next, we investigated the mechanism of I/R-induced loss of FMN by mitochondrial complex I. Previously, using the same *in vivo* model, we found 30-fold accumulation of succinate in the neonatal brain after HI (55). It has also been shown that oxidation of accumulated succinate by mitochondria stimulates RET, thereby affecting the redox state of complex I (10, 11, 61).

For further studies, we used intact brain mitochondria. First, we compared respiratory and H_2O_2 release activities of preparation from neonatal and adult (6–8 weeks) mice. Table 1 shows the quantitative characteristics of mitochondrial respiration and H_2O_2 release during forward or RET with malate/pyruvate or succinate/glutamate, respectively. We found that in comparison with adult animals, mitochondria from neonatal mice demonstrated slightly lower respiratory

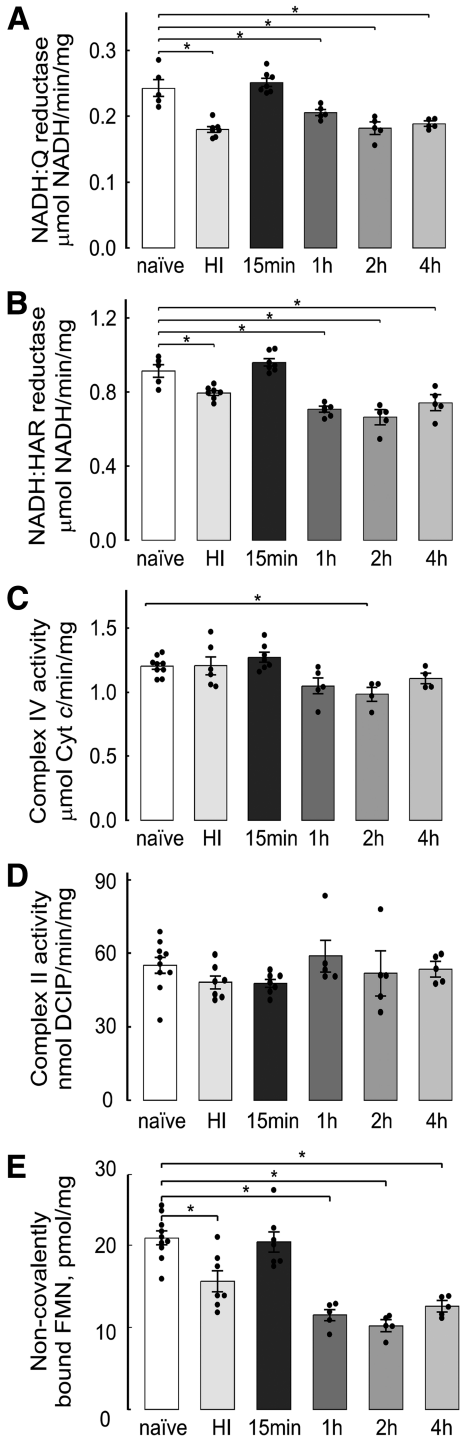

FIG. 2. Effect of HI-reperfusion on enzymatic activities of respiratory chain complexes and FMN content. (A) NADH:Q reductase activity of complex I; **(B)** NADH:HAR reductase activity of complex I; **(C)** ferrocytochrome *c* oxidase activity of complex IV; **(D)** succinate:DCIP reductase activity of complex II were measured in mitochondrial membranes; **(E)** content of noncovalently bound FMN in the mitochondrial membranes after HI-reperfusion. Mitochondrial fragments were isolated from the brain samples after HI as described in the Materials and Methods section. ($n = 4$–8 per group, $^*p < 0.05$, ANOVA with Dunnet's multiple-comparisons test). DCIP, 2,6-dichlorophenolindophenol; FMN, flavin mononucleotide; HAR, hexaammineruthenium (III).

Table 1. Respiration and H_2O_2 Release in Brain Mitochondria from Neonatal and Adult Mice

	Malate/pyruvate			*Succinate/glutamate*		
	Neonatal		*Adult*	*Neonatal*		*Adult*
H_2O_2 release rate, pmol H_2O_2/min/mg protein						
Nonphosphorylating	201 ± 15	*	143 ± 14	2187 ± 78	*	1748 ± 99
+0.2 m*M* ADP (state 3)	89 ± 7	*	55 ± 5	241 ± 33	*	142 ± 12
Respiration, nmol O_2/min/mg protein						
Nonphosphorylating	9 ± 2	*	15 ± 1	44 ± 2	*	52 ± 4
+0.2 m*M* ADP (state 3)	117 ± 6	*	140 ± 7	212 ± 12		242 ± 16
RCR	14.0 ± 3.5		9.5 ± 0.8	4.8 ± 0.2		4.7 ± 0.2

RCR, respiratory control ratio determined by the rate of state 3 respiration divided by the rate of nonphosphorylating respiration. *, significant difference between the means of neonatal and adult animals ($n = 8$ per group, $p < 0.05$, *t*-test) for the same conditions.

activity, but higher H_2O_2 release rate in both conditions ($n = 8$, $p < 0.05$, *t*-test).

It should be noted that in coupled mitochondria *in vitro*, succinate rapidly reduces the entire pool of matrix $NAD(P)^+$ nucleotides. Therefore, during the steady-state succinate oxidation, there is no reduction of $NAD(P)^+$ as originally defined in Chance and Hollunger (9) and upstream electron flow is now diverted to a different acceptor, that is, oxygen. We use the term RET-like conditions to describe the process of steady-state oxidation of succinate by coupled intact mitochondria.

Previously, using brain mitochondria from adult mice, we demonstrated that the rate of H_2O_2 release in RET-like conditions declines with time due to complex I inactivation (61). We tested whether this process occurs in mitochondria from neonatal mice. Figure 3A demonstrates representative traces of RET-induced H_2O_2 release rate by mitochondria obtained from animals of different ages. This process can be characterized by the half-time of the decay ($\tau_{1/2}$) of the H_2O_2 release rate, which was 3.5 ± 0.1 and 4.8 ± 0.1 min for mitochondria from the neonatal and adult mice, respectively (Fig. 3B). This indicates that RET-dependent decline of H_2O_2 release takes place faster in mitochondria from neonates.

We evaluated several parameters simultaneously with the decline of H_2O_2 release in neonatal mouse mitochondria oxidizing succinate in RET-like conditions (Fig. 4). First, we measured the fluorescence emission of mitochondrial flavins (Fig. 4B). We observed a rapid decrease of fluorescence intensity after addition of substrates, probably indicating a reduction of flavins. The initial decline was followed by a slow recovery of the fluorescence. This can reflect several processes such as release of the reduced flavin into the matrix followed by fast autoxidation by oxygen in the medium. A remarkable coincidence between the kinetics of fluorescence emission (Fig. 4B) and of H_2O_2 release rate (Fig. 4A) is evident. The flavin fluorescence emission corresponding to the flavin redox state (Fig. 4B) followed the inverted pattern of the decline of H_2O_2 release rate.

Next, we assessed the binding state of flavin in mitochondria during incubation in RET-like conditions. Aliquots were taken during incubation with succinate, the RET was stopped by addition of complex II inhibitor malonate, mitochondrial membranes were collected after a brief centrifugation, and supernatant and pellet were analyzed separately. Figure 4C shows a time course of concentration of soluble flavin in the supernatant and the residual content of non-covalently bound FMN in the membranes. An increase in the

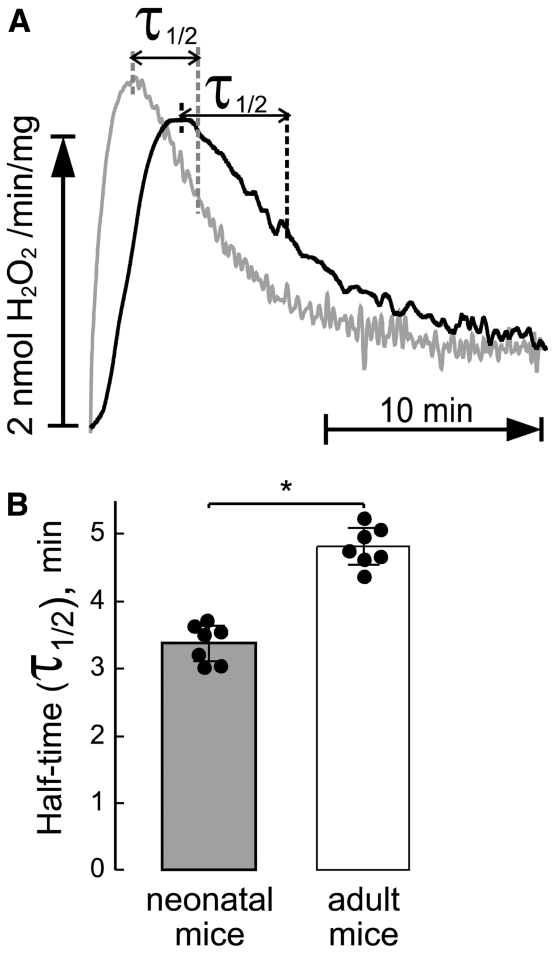

FIG. 3. Decline of H_2O_2 release in RET-like conditions. **(A)** Representative traces of H_2O_2 release by adult (*black*) and neonatal brain mitochondria (*gray*) during oxidation of succinate in RET-like conditions (5 m*M* succinate and 1 m*M* glutamate). Half-time ($\tau_{1/2}$) is defined as the time required to change the rate of H_2O_2 release by one-half during the rate decline; **(B)** comparison of the half-time of the H_2O_2 release rate decline in adult and neonatal brain mitochondria (*white* and *gray bars*, respectively, $n = 7$ per group, $^*p < 0.05$, *t*-test). RET, reverse electron transfer.

concentration of free flavin in the medium occurred simultaneously with a decrease of membrane-associated noncovalently bound FMN. Therefore, during incubation with succinate, the FMN dissociated from its binding site in the mitochondrial membrane, could go across the membrane, and was released to the outside.

Finally, we assessed activities of mitochondrial complex I (Fig. 4D). During incubation in RET-like conditions, small aliquots were taken and NADH-dependent activities of the enzyme were further assayed in permeabilized mitochondria. We found that both NADH:Q and NADH:HAR reductase activities decreased in parallel with the decline of H_2O_2 release rate (Fig. 4A) and decrease of noncovalently bound FMN in the membrane (Fig. 4C). These data indicate that, during incubation in RET-like conditions, complex I inactivation was taking place at the hydrophilic N-module.

No significant change in FMN fluorescence or H_2O_2 release was observed when mitochondria oxidized succinate in the presence of an uncoupler, a condition known to prevent RET (Fig. 5A). Gradual decrease of complex I NADH:Q reductase activity measured during incubation with succinate (Fig. 5B, solid squares) was also prevented if an uncoupler was present or if oxygen was absent (Fig. 5B, diamonds and solid triangles, respectively). RET is blocked in these conditions and, therefore, reduction and release of complex I FMN is prevented. Moreover, there was no complex I inactivation when mitochondria oxidized malate and pyruvate, substrates of NAD^+-dependent dehydrogenases that do not support RET (Fig. 5B, open triangles).

The data on FMN release to the incubation medium during succinate oxidation shown in Figure 4C suggest that the inner mitochondrial membrane is permeable to FMN. Therefore, we tested whether exogenously added flavin affects the RET-induced complex I inactivation. Figure 5B (open squares) demonstrates that the decline of complex I activity could be partially prevented if exogenous FMN was present during oxidation of succinate. Nonphosphorylated FMN precursor riboflavin was unable to prevent complex I inactivation (not shown).

Our results unequivocally demonstrate that oxidation of succinate by coupled mitochondria in RET-like conditions induced impairment of complex I due to the loss of FMN.

Effect of oxygen level on the decline of H_2O_2 release rate

Other important effectors of the RET reaction are the level of oxygen and ROS, which vary greatly on I/R. RET provides

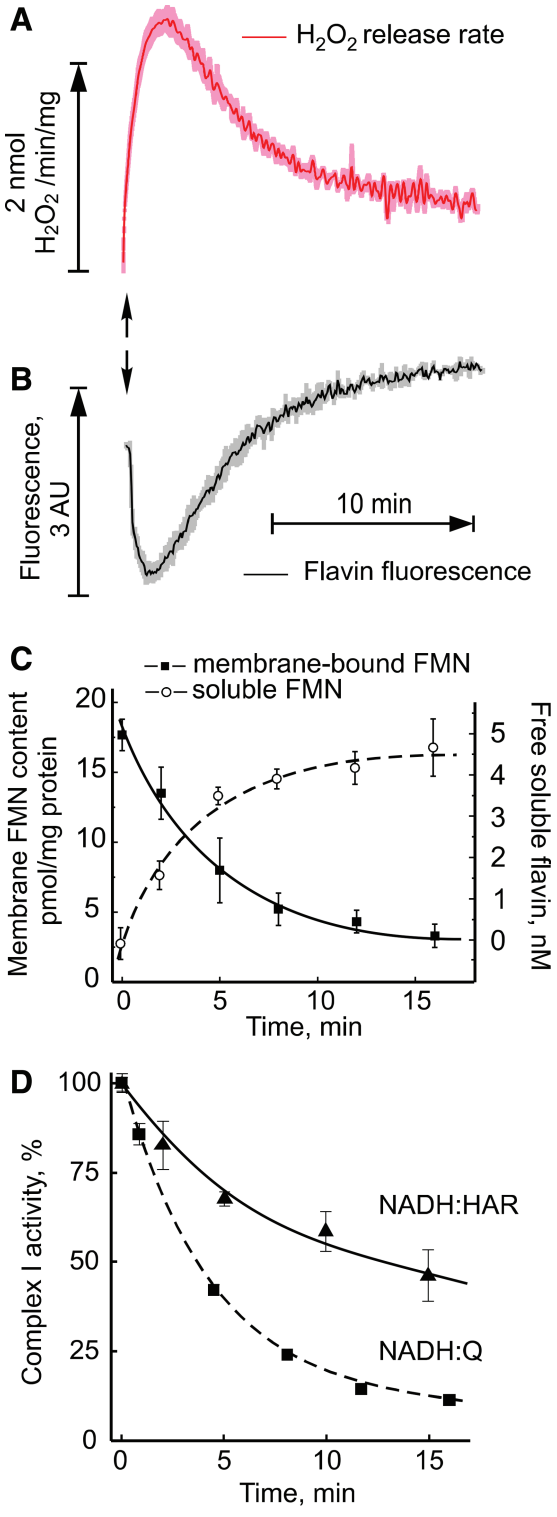

FIG. 4. Effect of incubation of neonatal intact brain mitochondria in RET-like conditions *in vitro*. (A) Representative trace of H_2O_2 release decline; **(B)** representative trace of flavin fluorescence emission at 525nm (excitation 460 nm); error bars represent one standard deviation based on triplicate measurements; **(C)** decrease of the content of membrane FMN and increase of concentration of free soluble flavin in the solution during incubation in RET-like conditions. Mitochondria (0.2 mg of protein/mL) were incubated as shown in Figure 3, 300-μL aliquots were taken in time, and membranes were separated by centrifugation. The content of membrane-bound FMN and concentration of free flavin was determined in pellet and supernatant, respectively, as described in the Materials and Methods section; **(D)** effect of incubation of intact brain mitochondria in RET-like conditions on NADH:HAR (*triangles*) and NADH:Q (*squares*) reductase activity of complex I. Mitochondria (0.1–0.3 mg of protein/mL) were incubated in the presence of substrates, small aliquots (50–110 μL) were taken in time, and complex I activities were assayed in permeabilized mitochondria as described in the Materials and Methods section. Addition of substrates is indicated by *arrows*. Color images are available online.

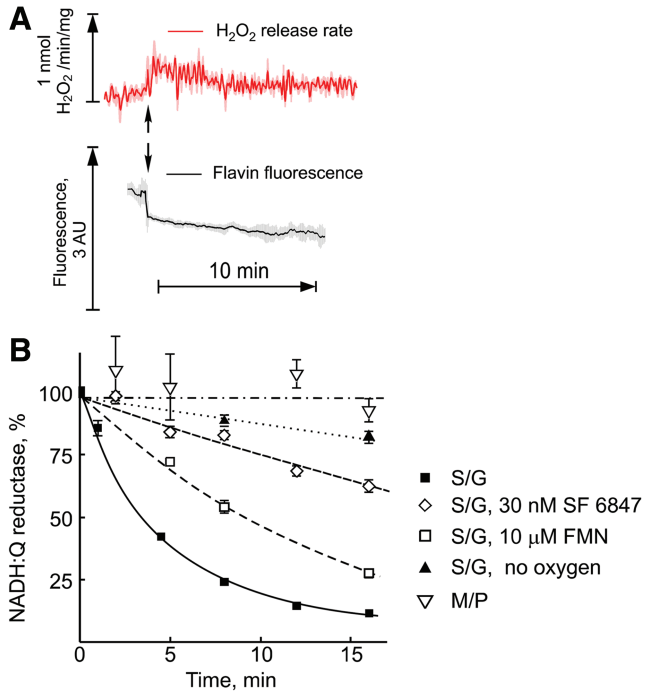

FIG. 5. Effect of RET-inhibition on H_2O_2 release, flavin fluorescence, and complex I inactivation in neonatal mitochondria incubated in RET-like conditions. (A) Representative traces of H_2O_2 release rate (*red*) and FMN fluorescence (*black*) in mitochondria oxidizing succinate in the presence of uncoupler SF 6847 (50 n*M*); **(B)** NADH:Q reductase activity decline during incubation with 5 m*M* succinate and 1 m*M* glutamate (S/G, no additions, *solid squares*), in the presence of 50 n*M* SF 6847 (*diamonds*), 10 μM FMN (*open squares*), or in anoxia (*solid triangles*). No complex I inactivation was observed during oxidation of 2 m*M* malate and 5 m*M* pyruvate (M/P, *open triangles*). Data from at least three independent experiments are shown. NADH:Q reductase activity was measured as shown in Figure 3D. Addition of substrates is shown by *arrows*. Color images are available online.

the highest rate of H_2O_2 release in mitochondria, with complex I as the main site of ROS production (11, 12, 19, 39, 40, 47, 49, 51, 61, 63, 70, 71). Data in Figure 6A demonstrate that the rate of H_2O_2 release during RET linearly depends on oxygen concentration. Therefore, the amount of endogenous ROS exposure during incubation with succinate can be modulated by oxygen level.

Using a Clark electrode-based gas-controlling system, we incubated intact brain mitochondria in RET-like conditions at different oxygen concentrations (Fig. 6B). The kinetics of complex I inactivation were estimated by using the half-life ($\tau_{1/2}$) of decline of H_2O_2 release rate (as in Fig. 3A). We found that the half-life of the decline was independent of oxygen concentration (Fig. 6C, open squares). After 16 min of incubation with succinate at different oxygen levels (10–200 μM O_2), the amount of endogenously produced H_2O_2 varied from 1 to 20 nmol H_2O_2/mg of protein (Fig. 6C, circles); however, no change in the rate of complex I inactivation was observed (Fig. 6D). It should be noted that we detected H_2O_2 released from the mitochondria to the outside and the local concentration in the matrix may be significantly higher. Hence, in our system, the decline of complex I activity was not due to possible oxidative ROS damage of the enzyme. This is a critical observation, suggesting that the mechanism of complex I impairment *via* FMN loss is different than the generally accepted mechanism of reperfusion-induced tissue injury by oxidative stress.

RET, supercomplexes assembly, and complex I integrity

FMN is noncovalently bound to the NDUFV1 subunit of complex I, located in the N-module of the hydrophilic arm protruding in the matrix. Thus, it is possible that FMN release during RET is due to the dissociation of the subunits composing the N-module. To monitor enzyme integrity, as well as supercomplexes assembly, we separated respiratory chain complexes by using blue native electrophoresis (BNE) and carried out complexome profiling (18, 27). We compared the abundance of all respiratory chain complexes' subunits between samples before and after incubation in RET-like conditions (Supplementary Tables S1 and S2). The heatmap (Fig. 7A–C) and resulting profiles (Fig. 7D) demonstrated that RET had very little effect on supercomplexes containing complex I. Individual complexes II-IV were also present at comparable levels (Supplementary Table S2). More importantly, the abundance of subunits of the hydrophilic N-module (Fig. 7E) and of the membrane P-module (Fig. 7F) were almost equal, indicating that there was no higher abundance of the enzyme subcomplex without the N-module. Therefore, we concluded that there is no evidence that RET *in vitro* leads to dissociation of complex I subunits around the NADH-binding site.

Riboflavin attenuates brain damage and preserves complex I activity in neonatal HI-reperfusion injury

Our results shown in Figures 2 and 5 generated a testable prediction. An increase in the tissue level of FMN precursor riboflavin should decrease the extent of brain I/R damage. Consecutive injections of riboflavin (25 mg/kg, total dose) before HI increased the concentration of soluble flavin in brain tissue almost twofold (Fig. 8A). As shown in Figure 8B, at 24 h after the insult, riboflavin-treated mice demonstrated a significantly decreased infarct volume compared with the vehicle-treated littermates. Sensorimotor reflex performance was significantly better in riboflavin-treated compared with vehicle-treated animals (Fig. 8C, D). Riboflavin pretreatment was associated with an increase of complex I activity at critical time-points after HI (Fig. 8E, F), suggesting a better preserved complex I.

Discussion

In this study, we sought to determine the mechanism of mitochondrial impairment in the neonatal model of brain I/R injury. Cerebral HI evoked an immediate effect on mitochondrial complex I, confirming earlier findings in immature (4, 33, 49) and mature (1, 2, 24, 28, 31, 57, 58) animals. Both physiological NADH:Q and artificial acceptor NADH:HAR reductase activities of the enzyme were affected. This implies a direct effect of I/R on the distal NADH dehydrogenase domain of the enzyme, where redox cofactors such as FMN and iron-sulfur clusters are located. Complex II (succinate

dehydrogenase) and complex IV (cytochrome *c* oxidase) were not significantly affected, supporting our previous observations in the brain HI model in rats (62) and mice (49). Complex I has a high degree of flux control over oxidative phosphorylation and can be considered the rate-limiting step of the respiratory chain (21, 41). Therefore, even minor changes in the activity of complex I could strongly influence the overall efficiency of ATP production and cellular bioenergetics after I/R. A rapid recovery of complex I activities after 15 min of reperfusion, followed by a secondary decline at 1 h of reperfusion, was not associated with significant effects on the rest of the respiratory chain. A similar biphasic pattern has been previously reported in the adult brain (49); however, the mechanisms for this secondary decline in the complex I-dependent mitochondrial respiration remained cryptic.

The content of noncovalently bound FMN in the mitochondrial membranes *ex vivo* changes with the same kinetics as complex I activity. After HI-induced decrease, FMN content was almost fully recovered after 15 min of reperfusion but then gradually declined after 1 h. The mammalian proteome comprises 15 FMN-containing proteins, of which only two enzymes are associated with mitochondria membrane and carry a noncovalently bound FMN (43). One of these enzymes is complex I and the other is dihydroorotate dehydrogenase, which has a much lower abundance in the brain tissue (56) [see also The Human Protein Atlas website (67)]. Since the main source of membrane-associated FMN is complex I and the decrease of complex I activity was correlated with loss of FMN, we concluded that the observed decrease in FMN content in HI-reperfusion is due to the loss of flavin cofactor from this enzyme. Flavin of complex I is noncovalently bound and is able to dissociate from the enzyme on reduction, as initially shown in the pioneering work of the Vinogradov's lab, using fragmented or intact mammalian enzyme (25, 60).

FMN release from complex I can be a secondary effect due to subunit dissociation from the N-module of the enzyme. In fact, recent studies showed that subunits of the matrix arm have a shorter lifetime than membrane subunits (P-module) (34). Our complexome profiling data of mitochondria from neonatal brain identified no significant change in complex I subunit abundance within supercomplexes or individual enzymes after RET *in vitro*. We compared the abundance of subunits close to the FMN-binding site (N-module) with

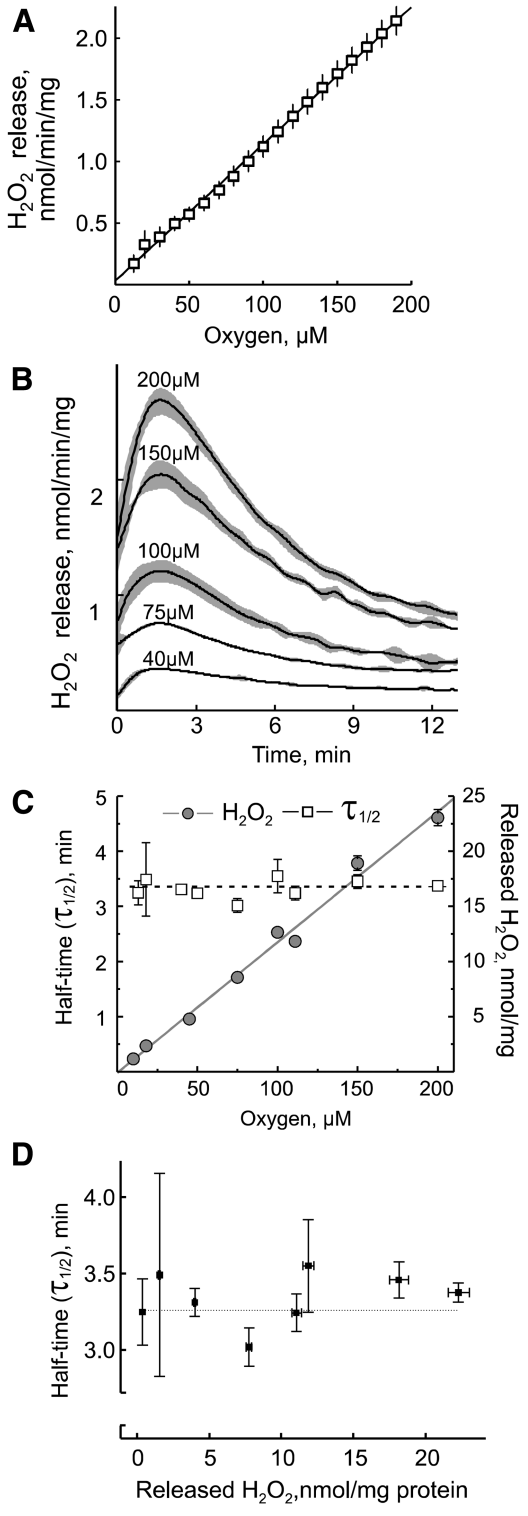

FIG. 6. Effect of oxygen concentration on kinetics of H_2O_2 release by neonatal brain mitochondria incubated in RET-like conditions. (A) Rates of H_2O_2 release during coupled oxidation of 5 m*M* succinate and 1 m*M* glutamate as a function of oxygen concentration ($n=6$). Oxygen concentration as measured directly by the Oroboros respirometer was rapidly varied by continuously purging the headspace with nitrogen as described in the Materials and Methods section; **(B)** representative traces of H_2O_2 release rate in RET-like conditions at various oxygen concentrations (from the *bottom* to the *top*, curves correspond to 40, 75, 100, 150, and 200 μM oxygen level during the assay). Oxygen concentration was controlled by purging the headspace of the reaction chamber with nitrogen/air mixture. Substrates were added at time zero. Error bars represent one standard deviation based on multiple measurements ($n=4$–5); **(C)** half-time of the H_2O_2 decline (*open squares*) and amount of released H_2O_2 (*circles*) measured at different oxygen concentrations ($n=4$–5 per oxygen concentration). Half-time values of an H_2O_2 rate decline ($\tau_{1/2}$) were determined as in Figure 3A; amount of exogenously released H_2O_2 was calculated as an area under the curve of H_2O_2 release rate between time-points 0 and 16 min. **(D)** Data of half-time values *versus* the amount of released H_2O_2 were obtained from Figure 6C.

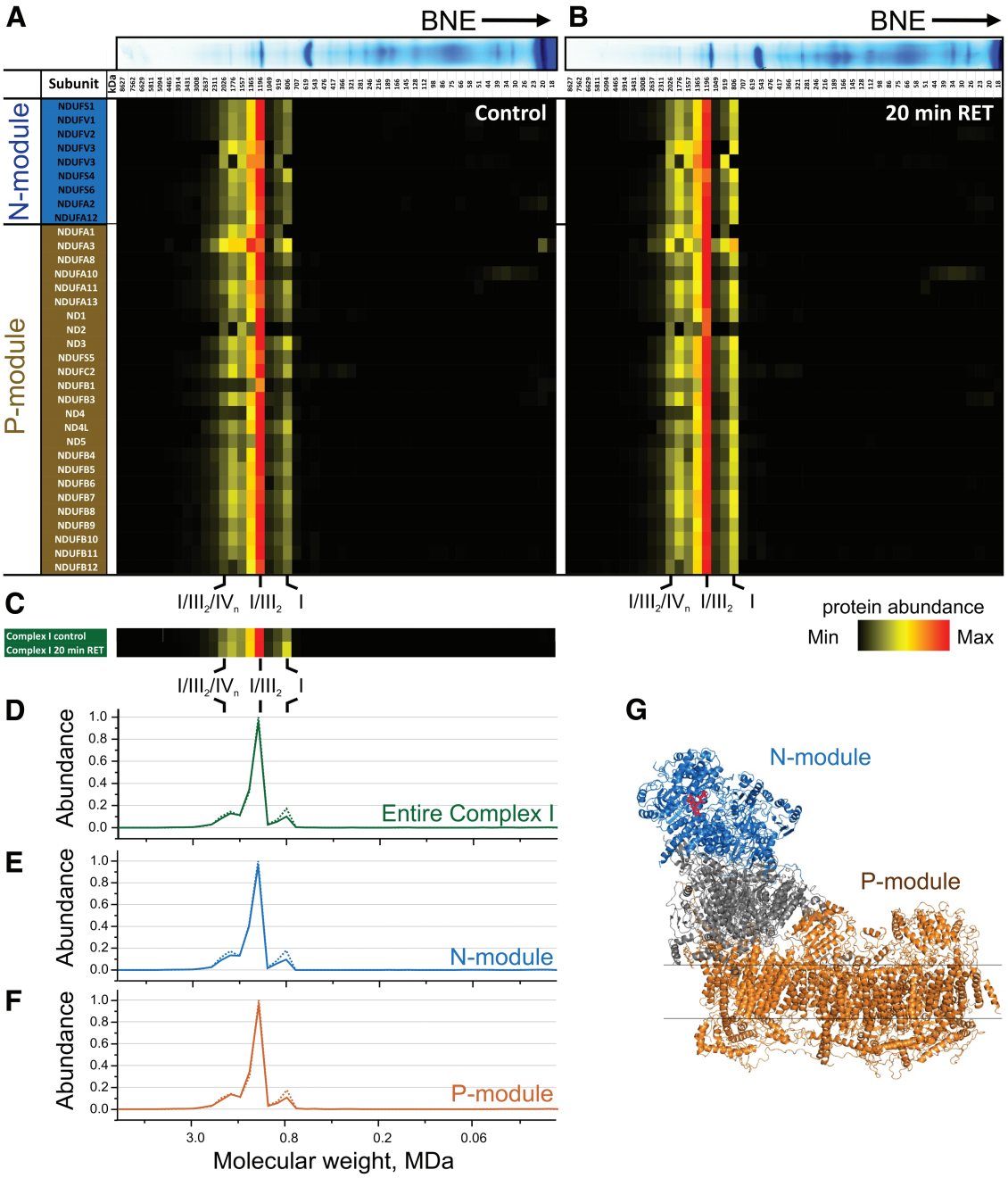

FIG. 7. Complexome profiling of mitochondria from neonatal brain. (A, B) Abundance of mitochondrial complex I proteins from untreated and RET-treated (20 min, conditions as in Fig. 3) membranes was normalized to maximal appearance and depicted in two heatmaps. Subunits of the peripheral N-module and membrane P-module are shown in *blue* and *tawny*, respectively. **(C)** Reference profiles (average of subunits) of complex I (*red*). **(D, E)** Reference profiles of the subunits of N- and P-modules (*blue* and *tawny*, respectively). Profiles of the untreated and RET-treated samples **(D–F)** are shown as *solid* and *dotted lines*. Assignment of complexes: I, complex I, I/III_2, supercomplex containing complex I and dimer of complex III; $I/III_2/IV_n$, supercomplex containing complex I, dimer of complex III, and one to four copies of complex IV. **(G)** Scheme of overall organization of mammalian complex I. The locations of peripheral subunits of N-module (*blue*) and membrane subunits of P-module (*tawny*) are shown in accordance to Zhu *et al.* (75). The FMN molecule (*red*) is noncovalently bound to the NDUFV1 subunit of the N-module. Color images are available online.

membrane-bound subunits (P-module). There is no higher abundance of complex I subcomplex without subunits of the N-module; therefore, FMN release is not due to complex I partial disintegration. In addition, no significant effect of RET on the supercomplexes assembly was found.

Recently, using a similar animal model of neonatal HI, we showed that succinate level spiked up to 30-folds after insult. It takes at least 30 min of reperfusion to return to the basal level (55) and during this time interval RET is expected to take place, as suggested by several earlier studies (10–12, 55,

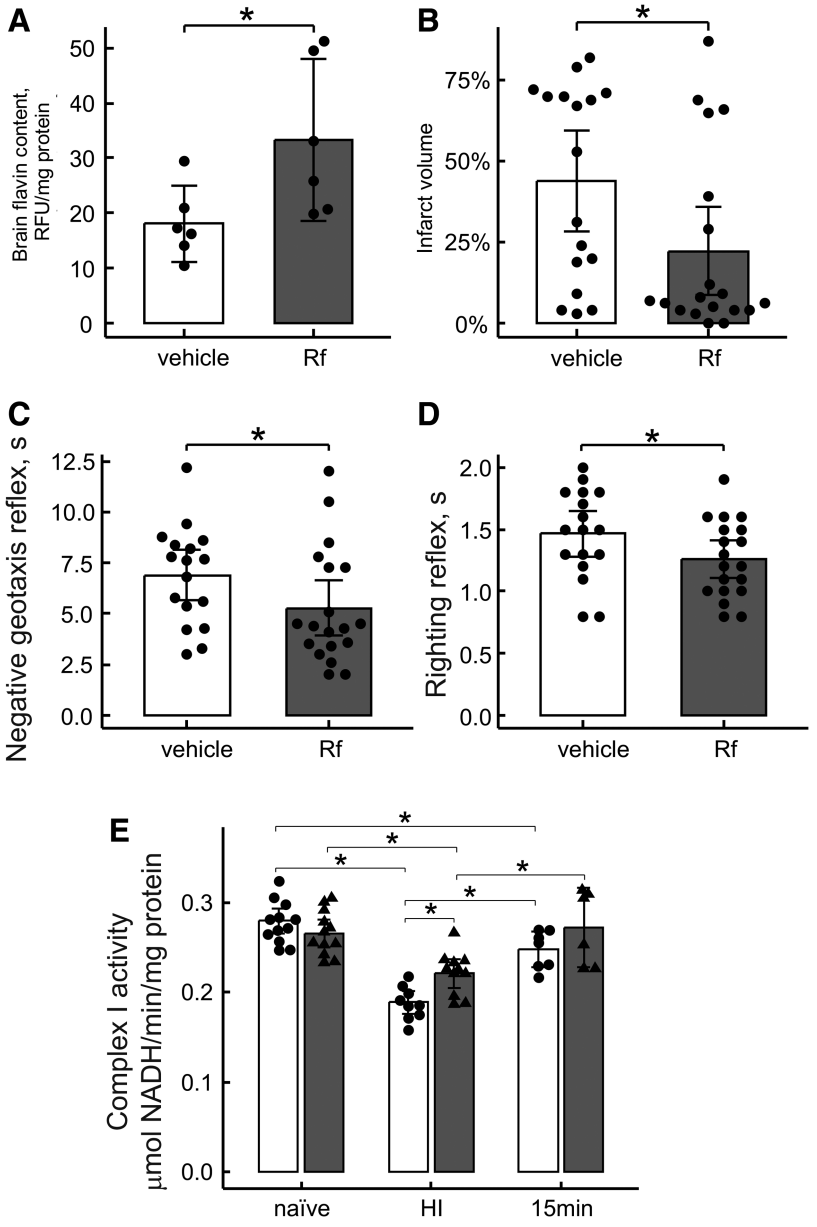

FIG. 8. Effect of riboflavin treatment on cerebral I/R injury after neonatal HI-reperfusion. **(A)** Total flavin concentration in the brain of vehicle- and riboflavin-treated mice (*white* and *gray bars*, respectively, $n = 6$ per group, $p < 0.05$, *t*-test); **(B)** infarct volume as a percentage of the hemisphere ($n = 17$–19 per group, $*p < 0.05$, Mann–Whitney test); **(C, D)** negative geotaxis and righting reflexes after HI-reperfusion in vehicle- and riboflavin-treated mice ($n = 11$–17, $*p < 0.05$, *t*-test); **(E)** complex I NADH:Q reductase activity measured in the samples obtained at critical time-points after HI only and 15 min after reperfusion of vehicle- and riboflavin-treated mice (*white* and *gray bars*, respectively, $n = 7$–12 per group, $*p < 0.05$, ANOVA with *t*-test with FDR correction for multiple comparison). FDR, false discovery rate.

62). Moreover, we reported a gradual RET-induced inactivation of complex I in brain mitochondria from adult animals (61). In this study, we determined that this process is significantly faster in mitochondria from the neonatal mice, probably due to the higher RET-induced H_2O_2 release. At an ambient oxygen concentration, RET-supported H_2O_2 release in the mitochondria from neonates was found to be 5.0% of the total electron flux whereas this was only 3.3% in adult mice (Table 1). This is most likely the reason for the faster decline of H_2O_2 rate in young animals when compared with adults (half-time of decline is 3.5 ± 0.1 and 4.8 ± 0.1 min, respectively).

In vitro, the kinetics of an H_2O_2 decline rate mirrored flavin fluorescence, indicating that the binding and redox state of the flavin changes during steady-state RET. We found that FMN was released from the membrane fraction and appeared in the incubation medium. FMN appearance in the solution coincided with the loss of both NADH:Q and NADH:HAR activities of complex I. In contrast to the physiological NADH:Q reductase, artificial NADH:HAR reductase activity was less affected by the incubation in RET-like conditions. It is possible that some fraction of the NADH:HAR-reductase in the neonatal tissue is not associated with mature complex I.

The FMN release and activity loss was prevented when RET was blocked by an uncoupler, which collapses the membrane potential required for the reverse flow of electrons from succinate to complex I. Anoxic reduction of respiratory chain by succinate was also insufficient for FMN dissociation, likely due to the same reason. Steady-state oxidation of substrates of NAD^+-dependent dehydrogenases such as malate and pyruvate did not inactivate the enzyme, indicating that reduction of the enzyme *ab imo* is a prerequisite for the fast FMN dissociation.

Since released FMN can penetrate the inner mitochondrial membrane, we hypothesized that exogenous flavin added to

the medium should protect complex I during incubation in RET-like conditions. Indeed, addition of 10 μM FMN (but not riboflavin) partially prevented complex I inactivation. Permeability of the mitochondrial membrane for FMN indicates that *in vitro*, this process is not compartmentalized only within mitochondria, but may also involve cellular cytoplasm.

Perhaps the most interesting problem concerning the FMN release from mitochondrial complex I during HI *in vivo* is the biphasic nature of the phenomenon. Why does FMN level in HI drop initially, then recover almost completely after 15 min of reperfusion, and finally drop again after 1 h? The most straightforward explanation stems from the fact that the enzyme gradually loses its FMN if reduced by NADH in conditions when electron transfer is blocked (25, 29, 31). Significant reduction of matrix $NAD(P)^+$ nucleotides during brain ischemia (32, 72, 73) would inevitably lead to the complex I flavin reduction and, therefore, partial dissociation. This process could explain the initial loss of FMN from complex I during HI. Reperfusion activates mitochondrial respiration, but since ADP/ATP ratio is high, mitochondria promptly use the membrane potential for ATP synthesis similarly to that in state 3 respiration. During this interval, free reduced FMN is being oxidized by oxygen and can rebind to complex I. After restoration of the energy balance to the basal level, the value of membrane potential is increased. Thus, further oxidation of accumulated succinate can now support RET driven by membrane potential. Shortly after reperfusion, these events set the conditions in which FMN dissociates from complex I for the second time.

Oxygen is necessary for the maintenance of RET in intact mitochondria whereas oxygen tension varies greatly in brain I/R. Confirming our recent finding in adult mice (61) and immature rat brain mitochondria (62), we showed that the rate of H_2O_2 release in RET depends linearly on oxygen concentration. Unexpectedly, the rate of RET-induced complex I inactivation was found to be independent of oxygen level and, consequently, on the amount of exogenously produced matrix ROS. This observation supports the possibility of this process *in vivo* during incomplete ischemia. Lack of oxygen in neonatal HI induces succinate accumulation (55) that can be oxidized by mitochondria supporting RET-like conditions even at very low oxygen. This differentiates the mechanism of RET-induced complex I inactivation found in this study from the commonly accepted model of oxidative stress damage in I/R.

We demonstrated that riboflavin administration increased total brain flavin level and this was associated with significant neuroprotection, which was concomitant with an increase of mitochondrial complex I activity. Reversibility of the RET-induced FMN dissociation opens a number of avenues to be pursued for therapeutic neuroprotective applications. Interestingly, it was shown that a high proportion of stroke patients manifested riboflavin deficiency after reperfusion (20). Together with a recent report of the clinical neuroprotective action of riboflavin in humans with focal stroke (14), our results warrant a sustained effort for the development of flavin-based interventions for I/R-related pathologies in the brain.

Materials and Methods

Sources of chemicals

Most of the chemicals were purchased from Sigma, including mannitol (#63559), sucrose (#84097), essentially fatty acid free bovine serum albumin (BSA, #A6003), NADH (#N8129), hexaammineruthenium (III) chloride (#262005), decylubiquinone (#D7911), digitonin (D141), and triphenyltetrazolium chloride (#T8877). Pierce BCA protein assay kit (#23225), Amplex UltraRed (#A36006), and horseradish peroxidase (#012001) were from Thermo Fisher Scientific. Alamethicin (#11425) and atpenin A5 (#11898) were from Cayman Chemical.

Neonatal cerebral HI injury

All studies were conducted according to protocols approved by the Columbia University Institutional Animal Care and Use Committee (IACUC). Transient HI was induced as described (46, 64). Seven-day-old C57BL/6J neonatal mice with their dams were purchased from Jackson Laboratories (Bar Harbor). HI brain injury was induced in mice at 10 days of age (p10) by permanent ligation of the right common carotid artery under isoflurane anesthesia. After 1.5 h of post-surgical recovery, mice were subjected to hypoxia (8% O_2/92% N_2; Tech Air, Inc., NY) for 15 min, at 37°C ± 0.5°C.

Immediately after HI or after a period of recirculation (15 min, 1, 2, 4 h), mice were decapitated, and heads were rapidly frozen in liquid nitrogen for further mitochondrial membrane preparation. At 24 h of reperfusion, another cohort of animals was used for assessment of the extent of cerebral infarcts and neurocognitive tests.

Riboflavin treatment protocol and study groups

Neonatal mice subjected to acute HI insult were pre- and post-treated with riboflavin (5 mg/kg, five intraperitoneal injections, at 24, 12, and 1.5 h before HI and at 0 and 1 h after reperfusion). Saline solution was used as a vehicle. Immediately after HI or after a period of recirculation as indicated, mice were decapitated and heads were immediately frozen in liquid nitrogen for further mitochondrial membrane preparation and activity measurements. At 24 h of reperfusion, another cohort of animals was used for assessment of the extent of cerebral infarcts and neurocognitive tests.

Measurement of infarct volume

At 24 h of reperfusion, mice were sacrificed; brains were harvested, sectioned into 1-mm-thick coronal slices, and stained with 2% TTC. Digital images of infarcted (white, no staining) and viable (red) areas of brains were traced (Adobe Photoshop 4.0.1) and analyzed (NIH image 1.62J). The extent of brain injury was expressed as a percentage of the hemisphere ipsilateral to the carotid artery ligation side.

Assessment of neonatal reflex performance

Two measures of neonatal mouse reflex performance were assessed 24 h after HI as described (64). For assessment of righting reflex performance, mice were placed in a supine position and the time in seconds required to flip to the prone position was recorded. Each animal was given three attempts, and the mean time to perform the reflex was recorded. For negative geotaxis reflex measurement, the animals were placed head downward on an inclined board (40°). The time required for the animal to rotate their bodies head up (>90° rotation) was recorded, up to a maximum observation time of 20 s; if the mouse was unable to perform the reflex within the

allotted time, the maximal time was assigned. Testing of all reflexes was done on a board covered with tightly stretched close-knit fabric, to ensure adequate friction.

Preparation of brain mitochondrial membranes for ex vivo *studies*

Mitochondrial membranes were isolated from frozen ipsilateral brain hemispheres by differential centrifugation. After sagittal transection of the frozen heads into two hemispheres, the regions with maximal damage were excised from the ipsilateral hemisphere cortex caudal to bregma level. Pieces of frozen brain tissue were homogenized with 60 strokes of tight pestle of 2 mL Kontes™ Dounce homogenizer in 1 mL of ice-cold isolation buffer mannitol/sucrose/ ethylene glycol-bis (β-aminoethyl ether)-*N*,*N*,*N*′,*N*′-tetraacetic acid (EGTA) medium (MSE) (225 m*M* mannitol, 75 m*M* sucrose, 20 m*M* HEPES-Tris, 1 m*M* EGTA, 1 mg/mL BSA, pH 7.4), containing 80 μg/mL alamethicin to release low-molecular-weight metabolites from mitochondria. Tissue debris was discarded after the centrifugation at 1500 *g* for 5 min at 4°C. The supernatant was centrifuged at 20,000 *g* for 15 min at 4°C, and the membrane pellet was washed twice with the isolation buffer without BSA. The final pellet was resuspended in 60 μL of the same buffer and stored at −80°C until use.

Isolation of intact brain mitochondria for in vitro *studies*

Intact brain mitochondria were isolated from neonatal or adult mice by differential centrifugation with digitonin treatment (53, 61). Forebrain hemispheres were excised and immediately immersed into ice-cold MSE buffer. One brain was homogenized with 40 strokes by tight pestle of a Dounce homogenizer in 10 mL of the MSE buffer, diluted twofold, and centrifuged at 5000 *g* for 4 min at 4°C in a refrigerated Beckman centrifuge. The supernatant was supplemented with 0.02% digitonin and centrifuged again at 10,000 *g* for 10 min. The pellet was then washed twice by centrifuging at 10,000 *g* for 10 min in MSE buffer without BSA. The final pellet was resuspended in 0.15 mL of washing buffer, supplemented with 2 mg/mL BSA, and stored on ice. At least three separate isolations were used for each experimental condition.

Measurement of respiratory chain enzyme activities in mitochondrial membranes

All activities were measured spectrophotometrically by using Molecular Devices SpectraMax M5 plate reader in 0.2 mL of the assay buffer (125 m*M* KCl, 20 m*M* HEPES-Tris, 0.02 m*M* EGTA, pH 7.6) at 25°C.

NADH-dependent activities of complex I were assayed as oxidation of 0.15 m*M* NADH at 340 nm ($\varepsilon_{340nm} = 6.22$ $mM^{-1}cm^{-1}$) in the assay buffer supplemented with 40 μg/mL alamethicin and 1 m*M* KCN (NADH media). NADH:Q reductase was measured in NADH media containing 2 mg/mL BSA, 60 μM decylubiquinone, and 5–15 μg protein per well. Only rotenone (1 μM) sensitive part of the activity was used for the calculations. NADH:HAR reductase was assayed in NADH media containing 1 m*M* HAR and 2–5 μg protein per well. One hundred percent corresponds to 0.35 ± 0.02 and 1.55 ± 0.04 μmol $NADH \times min^{-1} \times mg^{-1}$ for NADH:Q and NADH:HAR reductase, respectively.

Complex II succinate:DCIP reductase activity was recorded at 600 nm ($\varepsilon_{600nm} = 21$ $mM^{-1}cm^{-1}$) in the assay buffer containing 15 m*M* succinate, 40 μM decylubiquinone, 0.1 m*M* DCIP, 1 m*M* KCN, and 5–10 μg protein per well. Activity was fully sensitive to complex II inhibitor thenoyltrifluoroaceton.

Complex IV ferrocytochrome *c* oxidase activity was measured as oxidation of 50 μM ferrocytochrome *c* at 550 nm ($\varepsilon_{550nm} = 21.5$ $L \cdot mM^{-1}cm^{-1}$) in the assay buffer supplemented with 0.025% dodecylmaltoside and 1–3 μg protein per well. Activity was fully sensitive to 0.5 m*M* cyanide.

Measurement of respiration and mitochondrial H_2O_2 release in intact mitochondria

A respirometer (Oroboros), equipped with a home-built two-channel fluorescence optical setup, was used for simultaneous monitoring of oxygen concentration and fluorescence in 2 mL of mitochondrial suspension (61, 62). The fluorescent signal was calibrated by adding several aliquots of freshly made H_2O_2 (100–200 n*M*) at the end of the assay.

Mitochondria (0.1–0.3 mg of protein) were added to a 2-mL respiration buffer (125 m*M* KCl, 20 m*M* HEPES-Tris [pH 7.4], 0.02 m*M* EGTA, 4 m*M* KH_2PO_4, 2 m*M* $MgCl_2$, 2 mg/mL BSA), containing 10 μM Amplex UltraRed and 4 U/mL horseradish peroxidase. Substrates were 2 m*M* malate and 5 m*M* pyruvate or 5 m*M* succinate and 1 m*M* glutamate. To initiate a state 3 respiration (state 3), 200 μM ADP was added. All measurements were performed at 37°°. RET-like conditions were defined as prolonged (15–20 min) succinate-supported respiration.

To modulate the oxygen concentration in the respiring mitochondrial suspension, the 1-mL chamber headspace was continuously purged with humidified gaseous argon/air mixture at a rate of 10–60 mL/min. By varying the partial pressure of argon in the headspace, we were able to control oxygen concentration in the suspension. The time course of H_2O_2 release was measured for 15–20 min at different oxygen concentrations.

Determination of flavin content in riboflavin-treated mice

For extraction of riboflavin, the cortex of an entire frozen brain was rapidly excised, weighed, and stored at −80°C. Homogenization buffer (40 m*M* MES, 10 m*M* K-Pi, 1.2 m*M* EDTA, pH ~6.0, 0.02% digitonin) was added to the tissue in ratio 7 to 1. Tissue disintegration was performed with IKA Ultra-Turrax, T10, tissue disperser (setting 6) for 1 min. Tissue debris was discarded after centrifugation for 1 h at 80,000 *g* at 4°C. The resulting supernatant was filtered through Amicon filters with 3 kDa cutoff, and riboflavin fluorescence was measured in the resulting filtrate by using Hitachi F-7000 fluorospectrophotometer (excitation/emission 470/525 nm).

Determination of soluble and membrane-bound flavin in intact mitochondria

During incubation in RET-like condition, 300-μL aliquots containing 60 μg of mitochondrial protein were taken during incubation in RET-like conditions and 1-m*M* malonate was added to stop succinate oxidation. Membranes were quickly cooled and centrifuged at 15,000 *g* for 15 min at 4°C, and supernatant and pellet fractions were analyzed separately. Flavin fluorescence was measured by using Hitachi F-7000

fluorospectrophotometer (excitation/emission 470/525 nm). Freshly prepared standard solutions of FMN and flavin adenine dinucleotide (FAD) with known concentrations were used for calibration of fluorescence signal.

The concentration of flavin in the supernatant was measured as the difference in fluorescence emission before and after dithionite reduction of the 1:5 diluted supernatant in the 0.3-mL fluorometric cuvette.

To measure FMN content in the pellet, we used a modified protocol of Faeder and Siegel (16) based on different fluorescent emissions of FAD and FMN at different pH. Sixty micrograms of protein of the mitochondrial pellet was resuspended in 30 μL of water and mixed with 30 μL of 15% trichloroacetic acid for deproteinization as described earlier. To neutralize the supernatant, 9 μL of 4 *M* Tris was added (volumes were adjusted in preliminary experiments). Fluorescence emission was measured in 0.1 *M* Tris-HCl buffer containing 0.1 m*M* EDTA at two different pH (7.6 and 2.3). First, fluorescence at pH 7.6 was measured after the addition of 20 μL of sample into 0.3 mL of buffer; then, fluorescence at pH 2.3 was recorded after the addition of 40 μL of 1N HCl.

Determination of membrane-bound flavin ex vivo *after HI*

To measure FMN content in mitochondrial membranes after HI-reperfusion, we designed a plate reader-based protocol after (16, 37). Approximately 0.25 mg of mitochondria membrane protein was diluted with water to 1 mg/mL, mixed with an equal volume of 15% trichloroacetic acid, and incubated on ice for 10 min. Protein precipitate was removed by centrifugation at 10,000 *g* for 10 min. To partially neutralize the supernatant, a 1:10 volume of 4 *M* K_2HPO_4 (pH unadjusted) was added. Two hundred microliters was loaded into a well of a 96-well plate, and fluorescence under acidic conditions was recorded by using Molecular Devices SpectraMax M5 plate reader (excitation/emission 450/525 nm, auto PMT, 14 readings). After addition of 20 μL of 4 *M* K_2HPO_4, fluorescence under neutral conditions was recorded.

Blue native electrophoresis

Sample preparation and BNE of mitochondrial membranes were essentially done as described (74). Briefly, mitochondria (400 μg) were resuspended in 35-μL solubilization buffer (50 m*M* imidazole pH 7, 50 m*M* NaCl, 1 m*M* EDTA, 2 m*M* aminocaproic acid), solubilized with 10 μL 20% digitonin, and centrifuged for 20 min at 22,000 *g*. Supernatants were supplemented with 2.5 μL 5% Coomassie G250 in 500 m*M* aminocaproic acid and 5 μL 0.1% Ponceau S in 50% glycerol. Equal protein amounts of samples were loaded on top of a 3%–18% acrylamide gradient gel (dimension 14 × 14 cm). After native electrophoresis in a cold chamber, blue-native gels were fixed in 50% (v/v) methanol, 10% (v/v) acetic acid, and 10 m*M* ammonium acetate for 30 min and stained with Coomassie (0.025% Serva Blue G, 10% [v/v] acetic acid).

Sample preparation for complexome profiling

Each lane of a BNE gel was cut into 48 equal fractions and collected in 96-filter-well plates (30–40 μm PP/PE; Pall Corporation). The gel pieces were destained in 60% methanol, 50 m*M* ammoniumbicarbonate (ABC). Solutions were removed by centrifugation for 2 min at 600 *g*. Proteins were reduced in 10 m*M* DTT, 50 m*M* ABC for 1 h at 56°C and alkylated for 45 min in 30 m*M* iodoacetamid. Samples were digested for 16 h with trypsin (sequencing grade; Promega) at 37°C in 50 m*M* ABC, 0.01% Protease Max (Promega), and 1 m*M* $CaCl_2$. Peptides were eluted in 30% acetonitrile and 3% formic acid, centrifuged into a fresh 96-well plate, dried in a speed vac, and resolved in 1% acetonitrile and 0.5% formic acid.

Mass spectrometry for complexome profiling

Liquid chromatography/mass spectrometry (MS) was performed on a Thermo Scientific™ Q Exactive Plus equipped with an ultra-high-performance liquid chromatography unit (Thermo Scientific Dionex Ultimate 3000) and a Nanospray Flex Ion-Source (Thermo Scientific). Peptides were loaded on a C18 reversed-phase precolumn (Thermo Scientific) followed by separation with a 2.4 μm Reprosil C18 resin (Dr. Maisch GmbH) in-house packed picotip emitter tip (diameter 100 μm, 15 cm from New Objectives) by using a gradient from 4% acetonitrile, 0.1% formic acid to 50% eluent B (99% acetonitrile, 0.1% formic acid) for 30 min.

MS data were recorded by data-dependent acquisition. The full MS scan range was 300–2000 *m/z* with a resolution of 70,000, and an automatic gain control value of 3×10^6 total ion counts with a maximal ion injection time of 160 ms. Only higher charged ions (2+) were selected for MS/MS scans with a resolution of 17,500, an isolation window of 2 *m/z*, and an automatic gain control value set to 10^5 ions with a maximal ion injection time of 150 ms. MS1 Data were acquired in profile mode.

Data analysis

For data analysis, MaxQuant 1.6.1.0 (13) [19029910], NOVA (22), and Excel (Microsoft Office 2013) were used. Proteins were identified by using the mouse reference proteome database UniProtKB with 52538 entries, released in February 2018. Acetylation (+42.01) at the N-terminus and oxidation of methionine (+15.99) were selected as variable modifications, and carbamidomethylation (+57.02) was selected as fixed modification on cysteines. The enzyme specificity was set to Trypsin. False discovery rate (FDR) for the identification protein and peptides was 1%.

For complexome profiling, intensity-based absolute quantification values were recorded. The sum of all values from all protein IDs of treated samples (20 min RET) was used to normalize to control. Heatmap of proteins represents the abundance normalized to maximum appearance in a BNE lane. Slice number of the maximum appearance of mouse mitochondrial complex III dimer (483272 Da), complex IV (213172 Da), complex V (537939 Da), complex I (979577 Da), and respiratory supercomplex containing complex I, III dimer, and one copy of complex IV (1676021 Da) were used for native mass calibration.

Statistical analysis

Data analysis was performed by using R (version 3.5.1) in RStudio (Version 1.1.456, Boston, MA). All data are mean ± standard error of the mean. Statistically significant differences are indicated (*) when $p < 0.05$. Two-tailed *t*-test

or Mann–Whitney test was used to analyze intergroup differences between two groups. One-way ANOVA and Dunnet's test were used to compare groups after HI-reperfusion with the naive condition. For other comparisons between groups, multiple *t*-tests with FDR correction for multiple comparisons were used.

Acknowledgments

The authors would like to thank Prof. Andrei Vinogradov for a valuable discussion. They are grateful to Anna Bunin and Corey Anderson for help in the preparation of this article. They thank Jana Meisterknecht for excellent technical assistance for native electrophoresis and sample preparation for mass spectrometry. This study was supported by NIH grants NS100850 (V.T.), NS095692 (G.M.), and P01AG014930 for (A.A.S.); by the Deutsche Forschungsgemeinschaft: SFB 815/Z1 (I.W.); and by the BMBF mitoNET–German Network for Mitochondrial Disorders 01GM1906D (I.W.).

Author Disclosure Statement

No competing financial interests exist.

Supplementary Material

Supplementary Table S1
Supplementary Table S2

References

1. Allen KL, Almeida A, Bates TE, and Clark JB. Changes of respiratory chain activity in mitochondrial and synaptosomal fractions isolated from the gerbil brain after graded ischaemia. *J Neurochem* 64: 2222–2229, 1995.
2. Almeida A, Allen KL, Bates TE, and Clark JB. Effect of reperfusion following cerebral ischaemia on the activity of the mitochondrial respiratory chain in the gerbil brain. *J Neurochem* 65: 1698–1703, 1995.
3. Anderson MF and Sims NR. Mitochondrial respiratory function and cell death in focal cerebral ischemia. *J Neurochem* 73: 1189–1199, 1999.
4. Anderson MF and Sims NR. The effects of focal ischemia and reperfusion on the glutathione content of mitochondria from rat brain subregions. *J Neurochem* 81: 541–549, 2002.
5. Andreyev AY, Kushnareva YE, and Starkov AA. Mitochondrial metabolism of reactive oxygen species. *Biochemistry (Mosc)* 70: 200–214, 2005.
6. Birrell JA, Yakovlev G, and Hirst J. Reactions of the flavin mononucleotide in complex I: a combined mechanism describes NADH oxidation coupled to the reduction of $APAD^+$, ferricyanide, or molecular oxygen. *Biochemistry* 48: 12005–12013, 2009.
7. Canevari L, Kuroda S, Bates TE, Clark JB, and Siesjo BK. Activity of mitochondrial respiratory chain enzymes after transient focal ischemia in the rat. *J Cereb Blood Flow Metab* 17: 1166–1169, 1997.
8. Caspersen CS, Sosunov A, Utkina-Sosunova I, Ratner VI, Starkov AA, and Ten VS. An isolation method for assessment of brain mitochondria function in neonatal mice with hypoxic-ischemic brain injury. *Dev Neurosci* 30: 319–324, 2008.
9. Chance B and Hollunger G. Energy-linked reduction of mitochondrial pyridine nucleotide. *Nature* 185: 666–672, 1960.
10. Chouchani ET, Methner C, Nadtochiy SM, Logan A, Pell VR, Ding S, James AM, Cocheme HM, Reinhold J, Lilley KS, Partridge L, Fearnley IM, Robinson AJ, Hartley RC, Smith RA, Krieg T, Brookes PS, and Murphy MP. Cardioprotection by S-nitrosation of a cysteine switch on mitochondrial complex I. *Nat Med* 19: 753–759, 2013.
11. Chouchani ET, Pell VR, Gaude E, Aksentijevic D, Sundier SY, Robb EL, Logan A, Nadtochiy SM, Ord EN, Smith AC, Eyassu F, Shirley R, Hu CH, Dare AJ, James AM, Rogatti S, Hartley RC, Eaton S, Costa AS, Brookes PS, Davidson SM, Duchen MR, Saeb-Parsy K, Shattock MJ, Robinson AJ, Work LM, Frezza C, Krieg T, and Murphy MP. Ischaemic accumulation of succinate controls reperfusion injury through mitochondrial ROS. *Nature* 515: 431–435, 2014.
12. Cino M and Del Maestro RF. Generation of hydrogen peroxide by brain mitochondria: the effect of reoxygenation following postdecapitative ischemia. *Arch Biochem Biophys* 269: 623–638, 1989.
13. Cox J and Mann M. MaxQuant enables high peptide identification rates, individualized p.p.b.-range mass accuracies and proteome-wide protein quantification. *Nat Biotechnol* 26: 1367–1372, 2008.
14. da Silva-Candal A, Perez-Diaz A, Santamaria M, Correa-Paz C, Rodriguez-Yanez M, Arda A, Perez-Mato M, Iglesias-Rey R, Brea J, Azuaje J, Sotelo E, Sobrino T, Loza MI, Castillo J, and Campos F. Clinical validation of blood/brain glutamate grabbing in acute ischemic stroke. *Ann Neurol* 84: 260–273, 2018.
15. Edwards AD, Azzopardi DV, and Gunn AJ. *Neonatal Neural Rescue: A Clinical Guide*. Cambridge, United Kingdom: Cambridge University Press, 2013, 16 p.
16. Faeder EJ and Siegel LM. A rapid micromethod for determination of FMN and FAD in mixtures. *Anal Biochem* 53: 332–336, 1973.
17. Fiedorczuk K, Letts JA, Degliesposti G, Kaszuba K, Skehel M, and Sazanov LA. Atomic structure of the entire mammalian mitochondrial complex I. *Nature* 537: 644–648, 2016.
18. Fuhrmann DC, Wittig I, Drose S, Schmid T, Dehne N, and Brune B. Degradation of the mitochondrial complex I assembly factor TMEM126B under chronic hypoxia. *Cell Mol Life Sci* 75: 3051–3067, 2018.
19. Galkin A and Brandt U. Superoxide radical formation by pure complex I (NADH:ubiquinone oxidoreductase) from *Yarrowia lipolytica*. *J Biol Chem* 280: 30129–30135, 2005.
20. Gariballa S and Ullegaddi R. Riboflavin status in acute ischaemic stroke. *Eur J Clin Nutr* 61: 1237–1240, 2007.
21. Genova ML, Castelluccio C, Fato R, Parenti Castelli G, Merlo Pich M, Formiggini G, Bovina C, Marchetti M, and Lenaz G. Major changes in Complex I activity in mitochondria from aged rats may not be detected by direct assay of NADH: coenzyme Q reductase. *Biochem J* 311: 105–109, 1995.
22. Giese H, Ackermann J, Heide H, Bleier L, Drose S, Wittig I, Brandt U, and Koch I. NOVA: a software to analyze complexome profiling data. *Bioinformatics* 31: 440–451, 2015.
23. Gilland E, Puka-Sundvall M, Hillered L, and Hagberg H. Mitochondrial function and energy metabolism after hypoxia-ischemia in the immature rat brain: involvement of NMDA-receptors. *J Cereb Blood Flow Metab* 18: 297–304, 1998.
24. Ginsberg MD, Mela L, Wrobel-Kuhl K, and Reivich M. Mitochondrial metabolism following bilateral cerebral ischemia in the gerbil. *Ann Neurol* 1: 519–527, 1977.

25. Gostimskaya IS, Grivennikova VG, Cecchini G, and Vinogradov AD. Reversible dissociation of flavin mononucleotide from the mammalian membrane-bound NADH: ubiquinone oxidoreductase (complex I). *FEBS Lett* 581: 5803–5806, 2007.
26. Hansford RG, Hogue BA, and Mildaziene V. Dependence of H2O2 formation by rat heart mitochondria on substrate availability and donor age. *J Bioenerg Biomembr* 29: 89–95, 1997.
27. Heide H, Bleier L, Steger M, Ackermann J, Drose S, Schwamb B, Zornig M, Reichert AS, Koch I, Wittig I, and Brandt U. Complexome profiling identifies TMEM126B as a component of the mitochondrial complex I assembly complex. *Cell Metab* 16: 538–549, 2012.
28. Hillered L, Siesjo BK, and Arfors KE. Mitochondrial response to transient forebrain ischemia and recirculation in the rat. *J Cereb Blood Flow Metab* 4: 438–446, 1984.
29. Holt PJ, Efremov RG, Nakamaru-Ogiso E, and Sazanov LA. Reversible FMN dissociation from *Escherichia coli* respiratory complex I. *Biochim Biophys Acta* 1857: 1777–1785, 2016.
30. Hunte C, Zickermann V, and Brandt U. Functional modules and structural basis of conformational coupling in mitochondrial complex I. *Science* 329: 448–451, 2010.
31. Kahl A, Stepanova A, Konrad C, Anderson C, Manfredi G, Zhou P, Iadecola C, and Galkin A. Critical role of flavin and glutathione in Complex I-mediated bioenergetic failure in brain ischemia/reperfusion injury. *Stroke* 49: 1223–1231, 2018.
32. Kahraman S and Fiskum G. Anoxia-induced changes in pyridine nucleotide redox state in cortical neurons and astrocytes. *Neurochem Res* 32: 799–806, 2007.
33. Kim M, Stepanova A, Niatsetskaya Z, Sosunov S, Arndt S, Murphy MP, Galkin A, and Ten VS. Attenuation of oxidative damage by targeting mitochondrial complex I in neonatal hypoxic-ischemic brain injury. *Free Radic Biol Med* 124: 517–524, 2018.
34. Kim TY, Wang D, Kim AK, Lau E, Lin AJ, Liem DA, Zhang J, Zong NC, Lam MP, and Ping P. Metabolic labeling reveals proteome dynamics of mouse mitochondria. *Mol Cell Proteomics* 11: 1586–1594, 2012.
35. Knuuti J, Belevich G, Sharma V, Bloch DA, and Verkhovskaya M. A single amino acid residue controls ROS production in the respiratory complex I from *Escherichia coli*. *Mol Microbiol* 90: 1190–1200, 2013.
36. Korshunov SS, Skulachev VP, and Starkov AA. High protonic potential actuates a mechanism of production of reactive oxygen species in mitochondria. *FEBS Lett* 416: 15–18, 1997.
37. Kozioł J. Fluorometric analysis of riboflavin and its coenzymes. *Meth Enzymol* 18 B: 253–285, 1971.
38. Kristian T. Metabolic stages, mitochondria and calcium in hypoxic/ischemic brain damage. *Cell Calcium* 36: 221–233, 2004.
39. Kudin AP, Bimpong-Buta NY, Vielhaber S, Elger CE, and Kunz WS. Characterization of superoxide-producing sites in isolated brain mitochondria. *J Biol Chem* 279: 4127–4135, 2004.
40. Kussmaul L and Hirst J. The mechanism of superoxide production by NADH:ubiquinone oxidoreductase (complex I) from bovine heart mitochondria. *Proc Natl Acad Sci U S A* 103: 7607–7612, 2006.
41. Kuznetsov AV, Winkler K, Kirches E, Lins H, Feistner H, and Kunz WS. Application of inhibitor titrations for the detection of oxidative phosphorylation defects in saponin-skinned muscle fibers of patients with mitochondrial diseases. *Biochim Biophys Acta* 1360: 142–150, 1997.
42. Lee AC, Kozuki N, Blencowe H, Vos T, Bahalim A, Darmstadt GL, Niermeyer S, Ellis M, Robertson NJ, Cousens S, and Lawn JE. Intrapartum-related neonatal encephalopathy incidence and impairment at regional and global levels for 2010 with trends from 1990. *Pediatr Res* 74(Suppl 1): 50–72, 2013.
43. Lienhart WD, Gudipati V, and Macheroux P. The human flavoproteome. *Arch Biochem Biophys* 535: 150–162, 2013.
44. Liu Y, Fiskum G, and Schubert D. Generation of reactive oxygen species by the mitochondrial electron transport chain. *J Neurochem* 80: 780–787, 2002.
45. Lorek A, Takei Y, Cady EB, Wyatt JS, Penrice J, Edwards AD, Peebles D, Wylezinska M, Owen-Reece H, and Kirkbride V. Delayed (''secondary'') cerebral energy failure after acute hypoxia-ischemia in the newborn piglet: continuous 48-hour studies by phosphorus magnetic resonance spectroscopy. *Pediatr Res* 36: 699–706, 1994.
46. Mayurasakorn K, Niatsetskaya ZV, Sosunov SA, Williams JJ, Zirpoli H, Vlasakov I, Deckelbaum RJ, and Ten VS. DHA but not EPA emulsions preserve neurological and mitochondrial function after brain hypoxia-ischemia in neonatal mice. *PLoS One* 11: e0160870, 2016.
47. Murphy MP. How mitochondria produce reactive oxygen species. *Biochem J* 417: 1–13, 2009.
48. Nakai A, Kuroda S, Kristian T, and Siesjo BK. The immunosuppressant drug FK506 ameliorates secondary mitochondrial dysfunction following transient focal cerebral ischemia in the rat. *Neurobiol Dis* 4: 288–300, 1997.
49. Niatsetskaya ZV, Sosunov SA, Matsiukevich D, Utkina-Sosunova IV, Ratner VI, Starkov AA, and Ten VS. The oxygen free radicals originating from mitochondrial complex I contribute to oxidative brain injury following hypoxia-ischemia in neonatal mice. *J Neurosci* 32: 3235–3244, 2012.
50. Puka-Sundvall M, Gajkowska B, Cholewinski M, Blomgren K, Lazarewicz JW, and Hagberg H. Subcellular distribution of calcium and ultrastructural changes after cerebral hypoxia-ischemia in immature rats. *Brain Res Dev Brain Res* 125: 31–41, 2000.
51. Quinlan CL, Perevoshchikova IV, Hey-Mogensen M, Orr AL, and Brand MD. Sites of reactive oxygen species generation by mitochondria oxidizing different substrates. *Redox Biol* 1: 304–312, 2013.
52. Rao NA, Felton SP, Huennekens FM, and Mackler B. Flavin mononucleotide: the coenzyme of reduced diphosphopyridine nucleotide dehydrogenase. *J Biol Chem* 238: 449–455, 1963.
53. Rosenthal RE, Hamud F, Fiskum G, Varghese PJ, and Sharpe S. Cerebral ischemia and reperfusion: prevention of brain mitochondrial injury by lidoflazine. *J Cereb Blood Flow Metab* 7: 752–758, 1987.
54. Rousset CI, Baburamani AA, Thornton C, and Hagberg H. Mitochondria and perinatal brain injury. *J Matern Fetal Neonatal Med* 25(Suppl 1): 35–38, 2012.
55. Sahni PV, Zhang J, Sosunov S, Galkin A, Niatsetskaya Z, Starkov A, Brookes PS, and Ten VS. Krebs cycle metabolites and preferential succinate oxidation following neonatal hypoxic-ischemic brain injury in mice. *Pediatr Res* 83: 491–497, 2017.
56. Schaefer CM, Schafer MK, and Lofflerr M. Region-specific distribution of dihydroorotate dehydrogenase in the rat

central nervous system points to pyrimidine de novo synthesis in neurons. *Nucleosides Nucleotides Nucleic Acids* 29: 476–481, 2010.
57. Sims NR. Selective impairment of respiration in mitochondria isolated from brain subregions following transient forebrain ischemia in the rat. *J Neurochem* 56: 1836–1844, 1991.
58. Sims NR and Pulsinelli WA. Altered mitochondrial respiration in selectively vulnerable brain subregions following transient forebrain ischemia in the rat. *J Neurochem* 49: 1367–1374, 1987.
59. Sled VD and Vinogradov AD. Kinetics of the mitochondrial NADH-ubiquinone oxidoreductase interaction with hexammineruthenium(III). *Biochim Biophys Acta* 1141: 262–268, 1993.
60. Sled VD and Vinogradov AD. Reductive inactivation of the mitochondrial three subunit NADH dehydrogenase. *Biochim Biophys Acta* 1143: 199–203, 1993.
61. Stepanova A, Kahl A, Konrad C, Ten V, Starkov AS, and Galkin A. Reverse electron transfer results in a loss of flavin from mitochondrial complex I: potential mechanism for brain ischemia reperfusion injury. *J Cereb Blood Flow Metab* 37: 3649–3658, 2017.
62. Stepanova A, Konrad C, Guerrero-Castillo S, Manfredi G, Vannucci S, Arnold S, and Galkin A. Deactivation of mitochondrial complex I after hypoxia-ischemia in the immature brain. *J Cereb Blood Flow Metab* 2018. [Epub ahead of print]; DOI: 10.1177/0271678X18770331.
63. Tahara EB, Navarete FD, and Kowaltowski AJ. Tissue-, substrate-, and site-specific characteristics of mitochondrial reactive oxygen species generation. *Free Radic Biol Med* 46: 1283–1297, 2009.
64. Ten VS, Bradley-Moore M, Gingrich JA, Stark RI, and Pinsky DJ. Brain injury and neurofunctional deficit in neonatal mice with hypoxic-ischemic encephalopathy. *Behav Brain Res* 145: 209–219, 2003.
65. Ten VS, Yao J, Ratner V, Sosunov S, Fraser DA, Botto M, Sivasankar B, Morgan BP, Silverstein S, Stark R, Polin R, Vannucci SJ, Pinsky D, and Starkov AA. Complement component c1q mediates mitochondria-driven oxidative stress in neonatal hypoxic-ischemic brain injury. *J Neurosci* 30: 2077–2087, 2010.
66. Thornton C, Rousset CI, Kichev A, Miyakuni Y, Vontell R, Baburamani AA, Fleiss B, Gressens P, and Hagberg H. Molecular mechanisms of neonatal brain injury. *Neurol Res Int* 2012: 506320, 2012.
67. Thul PJ, Akesson L, Wiking M, Mahdessian D, Geladaki A, Ait Blal H, Alm T, Asplund A, Bjork L, Breckels LM, Backstrom A, Danielsson F, Fagerberg L, Fall J, Gatto L, Gnann C, Hober S, Hjelmare M, Johansson F, Lee S, Lindskog C, Mulder J, Mulvey CM, Nilsson P, Oksvold P, Rockberg J, Schutten R, Schwenk JM, Sivertsson A, Sjostedt E, Skogs M, Stadler C, Sullivan DP, Tegel H, Winsnes C, Zhang C, Zwahlen M, Mardinoglu A, Ponten F, von Feilitzen K, Lilley KS, Uhlen M, and Lundberg E. A subcellular map of the human proteome. *Science* 356: eaal3321, 2017.
68. Vannucci RC and Vannucci SJ. A model of perinatal hypoxic-ischemic brain damage. *Ann N Y Acad Sci* 835: 234–249, 1997.
69. Varghese F, Atcheson E, Bridges HR, and Hirst J. Characterization of clinically identified mutations in NDUFV1, the flavin-binding subunit of respiratory complex I, using a yeast model system. *Hum Mol Genet* 24: 6350–6360, 2015.
70. Vinogradov AD and Grivennikova VG. Generation of superoxide-radical by the NADH:ubiquinone oxidoreductase of heart mitochondria. *Biochemistry (Mosc)* 70: 120–127, 2005.
71. Votyakova TV and Reynolds IJ. $\Delta\Psi_m$-dependent and -independent production of reactive oxygen species by rat brain mitochondria. *J Neurochem* 79: 266–277, 2001.
72. Welsh FA, Marcy VR, and Sims RE. NADH fluorescence and regional energy metabolites during focal ischemia and reperfusion of rat brain. *J Cereb Blood Flow Metab* 11: 459–465, 1991.
73. Welsh FA, Sakamoto T, McKee AE, and Sims RE. Effect of lactacidosis on pyridine nucleotide stability during ischemia in mouse brain. *J Neurochem* 49: 846–851, 1987.
74. Wittig I and Braun HP, Schägger H. Blue native PAGE. *Nat. Protoc* 1: 418–428, 2006.
75. Zhu J, Vinothkumar KR, and Hirst J. Structure of mammalian respiratory complex I. *Nature* 536: 354–358, 2016.

Address correspondence to:
Dr. Alexander Galkin
Division of Neonatology
Department of Pediatrics
Columbia University
William Black Building
650 W 168th Street
New York, NY 10032

E-mail: ag4003@cumc.columbia.edu

Date of first submission to ARS Central, November 14, 2018; date of final revised submission, April 26, 2019; date of acceptance, April 29, 2019.

Abbreviations Used

ABC = ammoniumbicarbonate
BNE = blue native electrophoresis
BSA = bovine serum albumin
DCIP = 2,6-dichlorophenolindophenol
EGTA = ethylene glycol-bis(β-aminoethyl ether)-*N*,*N*,*N*′,*N*′-tetraacetic acid
FAD = flavin adenine dinucleotide
FDR = false discovery rate
FMN = flavin mononucleotide
HAR = hexaammineruthenium (III)
HI = hypoxia-ischemia
I/R = ischemia/reperfusion
MS = mass spectrometry
MSE = mannitol/sucrose/EGTA medium
Q = ubiquinone
RCR = respiratory control ratio
RET = reverse electron transfer
ROS = reactive oxygen species
TTC = triphenyltetrazolium chloride